EGYPTIAN ACADEMIC JOURNAL OF
BIOLOGICAL SCIENCES
ENTOMOLOGY

A

ISSN
1687-8809

WWW.EAJBS.EG.NET

Vol. 17 No. 3 (2024)

Citation: *Egypt. Acad. J. Biolog. Sci. (A. Entomology) Vol. 17(3) pp.51-67 (2024)*
DOI: 10.21608/EAJBSA.2024.374781

Egypt. Acad. J. Biolog. Sci., 17(3):51-67 (2024)

E**gyptian Academic Journal of Biological Sciences**
A. Entomology

ISSN 1687- 8809
http://eajbsa.journals.ekb.eg/

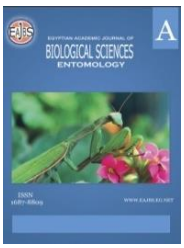

Ecofriendly Control of The Filarial Vector, *Culex pipiens* (Diptera; Culicidae) Using Green Synthesized Silver Nanoparticles

Mohamed A. Ahmed [1], Kotb M. Hammad [1], Mohamed A. Awad [1]and Amr Fouda [2]

[1]Department of Zoology and Entomology, Faculty of Science, Al-Azhar University, Cairo 11884, Egypt.

[2]Department of Botany and Microbiology, Faculty of Science, Al-Azhar University, Cairo 11884, Egypt.

*E-mail: awedm713@gmail.com

ARTICLE INFO

Article History
Received:15/7/2024
Accepted:19/8/2024
Available:23/8/2024

Keywords:
Biogenic; Ag-NPs; *Culex pipens*, larvicidal.

ABSTRACT

Nanotechnology is a trend that highly advanced over the past thirty years, addressing and resolving more challenges across different fields. In this investigation, biogenic silver nanoparticles (Ag-NPs) were formed using *Brevibacillus agri* as an endophytic bacterial strain and utilized as a safe approach to control the spread of medical insect, *Culex pipens*. The formed Ag-NPs were characterized by UV-vis analysis that showed maximum surface plasmon resonance at a wavenumber of 420 nm. Fourier transforms infrared analysis exhibits the role of various biomolecules in bacterial filtrate reduction and capping as-formed NPs. The sizes of biogenic NPs were 20 – 50 nm with spherical shapes with weight and atomic percentages of Ag ions of 46.20% and 13.96% respectively as shown by SEM-EDX analysis. The crystalline structure was confirmed by XRD. The mortality of various instar larvae and pupae of *C. pipens* were concentration-dependent and showed maximum percentages of 88.4±0.95, 76.3±0.8, 69.6±1.1, 52.1±1.4, and 47.3±1.01% for first to fourth instar larvae and pupae respectively at a concentration of 30 ppm. The concentrations of proteins, carbohydrates, and lipids of III instar larvae were decreased from (172.1 ± 4.31, 118.1±4.6, and 463.1±1.32 µg/g) for the control to (54.2±1.72, 91.3±2.17, 204.6±9.31 µg/g) respectively upon treatment with 30 ppm of Ag-NPs.

INTRODUCTION

Numerous human diseases are spread by the *Culex* mosquito, particularly in tropical and metropolitan areas. Elephantiasis, also known as lymphatic filariasis, is a disease that is spread to humans by mosquitoes and results in covert lymphatic system damage that can permanently disable a person (Organization, 2016). At this time, 1.5 billion people in approximately 73 nations are infected with lymphatic filariasis, putting them at risk of infection (Al-Kubati, Al-Samie, Al-Kubati, & Ramzy, 2020). Moreover, the current Zika virus epidemics that have been reported in the Caribbean, Central America, and South America are the result of the fourth and most recent arrival of arboviruses in the Western Hemisphere. These arboviruses do not have a specific treatment (Benelli & Mehlhorn, 2016). After the emergence of the Zika virus, the West Nile virus surfaced in 1999, Chikungunya

appeared in 2013, and Dengue, which had been subtly proliferating throughout the hemisphere for decades, intensified its spread in the 1990s (Benelli & Mehlhorn, 2016). China is among the nations where filariasis poses a health risk, and its government has been making great efforts to stop the disease's spread throughout all of its provinces (De-Jian, Xu-Li, & Ji-Hui, 2013). Typically, microbiological agents, regulators of insect growth, and organophosphates are used to target mosquito larvae. In actuality, the environment and human health are negatively impacted by these pollutants.

Recently, safe and effective methods such as mosquitocidal nanoparticles (MNP) and the sterile insect technique (SIT) have been created to better combat mosquitoes. The dengue vector *Aedes aegypti*, the filariasis mosquito *Culex quiquefasciatus*, and the malaria vector *Anopheles stephensi* are all severely poisoned by a few parts per million of various MNP. Nonetheless, despite mounting evidence of MNP's effectiveness, only modest attempts have been made to highlight the potential non-target effects of the chemical on aquatic organisms and the natural enemies of mosquitoes (Benelli, 2015; Muthukumaran, Govindarajan, Rajeswary, & Hoti, 2015). Biological organisms, such as *Bacillus* species, which are well-known for their impact on mosquito larvae, have been utilized in mosquito control efforts for a long time.

The two that work best against *Culex* mosquitoes are *Bacillus* spp. including *B. sphaericus* and *B. thuringiensis* (Soni & Prakash, 2014). Researchers are focusing on the need to develop new insecticides, such as silver nanoparticles (Ag-NPs), due to the rise in insect resistance to chemical pesticides and toxicity issues (Panneerselvam, Murugan, Kovendan, Kumar, & Subramaniam, 2013; Roni *et al.,* 2015; Santhosh, Ragavendran, & Natarajan, 2015).

A common bacterial endophyte that infects a lot of plants, *Bacillus amyloliquefaciens* has drawn a lot of attention for helping plants become more resistant to diseases. Crude lipopeptides made from *B. amyloliquefaciens* cultures have been shown to have antagonistic activity against three different types of pathogens (Chen *et al.,* 2013; Li, Soares, Torres, Bergen, & White Jr, 2015).

Biocontrol-active *B. amyloliquefaciens* and *B. subtilis* isolate yield a variety of antimicrobial CLP and control of Land Pollution such as fengycin, iturin A, and surfactin. In addition to their effect on insect pests, the metabolites also possess antifungal and antibacterial properties that influence the movement of bacteria and the production of biofilms (Chowdhury, Hartmann, Gao, & Borriss, 2015; Nam, Yang, Oh, Anderson, & Kim, 2016). In the twenty-first century, agriculture depends on the prevention of plant diseases. Microorganisms have caused substantial losses for farmers and are linked to a number of deadly illnesses that affect economically significant crops globally. *Xanthomonas oryzae* pv. *oryzae* (Xoo), one of the microbes that cause rice leaf blight, is the one that causes the most economic loss.

It is most severe in Asia and has been documented to occur in all rice-growing regions. According to reports, BLB can significantly impact yield losses in tropical regions of Asia, reaching up to 50 or 60% (Van Hop *et al.,* 2014). Thus, the key to maintaining rice yield is lowering the annual disease rate and the pace at which epidemics occur. These days, it's quite difficult to control sickness because most germs have become resistant to bactericidal agents. Preventing the disease's spread to uninfected plants was the main goal of the present control methods. Nanoparticles for the management of plant diseases have garnered a lot of attention in recent studies. The present study aimed at evaluating. The activity of silver nanoparticles synthesized using Fungi and Bactria against *Culex pipiens* in different stages, The activity of copper nanoparticles synthesized using Fungi and Bactria against *Culex pipiens* in different stages. The activity of silver and Copper nanoparticles synthesized using Fungi and Bactria against *Culex pipiens* at different stages.

MATERIALS AND METHODS

Bacterial Strain:

The endophytic bacterial strain *Brevibacillus agri* strain Af.15 was employed for the biosynthesis of Ag-NPs. This strain was originally isolated from the medicinal plant *Achillea fragrantissima*, collected from Wadi Selebat in the Saint Katherine Protectorate, South Sinai, Egypt. The sequence obtained for bacterial strain Af.15 has been added in GenBank with number of KY555795 (Alkahtani *et al.,* 2020).

Biosynthesis of Ag-NPs:

The nutrient broth media was used to inoculate the strain Af.15 before incubation under a shaking state at 35 ± 2°C for 24 h followed by centrifugation for ten minutes at 7000 rpm to harvest the cells. After that, the sterilized distilled water (dH_2O) was used to wash collected cells before being resuspension into 100 mL of dH_2O for 24 h. followed by filter paper filtration to collect the filtrate (cell-free filtrate, CFF). Finally, the collected CFF was used as a biocatalyst for the reduction of metal precursor ($AgNO_3$) to form Ag-NPs as follows: 1 mM of $AgNO_3$ was added to 100 mL of CFF under stirring conditions at 50°C for 2h. During stirring, the pH of the mixture was adjusted at 8 using 1 N NaOH which added drop wisely. The mixture was kept at room temperature in dark conditions till completely formed of yellowish-brown colour which refers to Ag-NP formation (Alsharif et al., 2020). The resultant was dried overnight at 100°C to collect the residue. The CFF and $AgNO_3$ aqueous solution were used as a negative control.

Ag-NPs Characterization:

UV-Visible Spectrophotometry:

UV-visible spectrophotometric analysis was conducted using a JENWAY 6305 Spectrophotometer to evaluate the optical features of the biosynthesized nano-Ag. The colour of the nano-solution was investigated in the range of 300 – 700 nm, with 10 nm intervals (Sher *et al.,* 2022). To confirm the occurrence of this colour change indicative of Ag-NPs formation, the blank for the JENWAY spectrophotometer consisted of the CFF of the endophytic bacterial strain.

Morphological and Elemental Mapping Investigations:

The morphological feature of bacterial synthesized Ag-NPs was assessed using scanning electron microscopy (JEOL, JSM-6360LA, Japan). The sample was prepared by fixing it onto a conductive substrate and coating it with a thin layer of gold. Once prepared, the sample is placed in the vacuum chamber of the SEM. Electron beams are then directed at the sample surface, and secondary electrons emitted from the sample are detected. The interaction between the electrons and the sample provides detailed information about its surface morphology. The SEM was connected with an Energy Dispersive Spectroscopy (EDX) unit to detect the elementary mapping of synthesized Ag-NPs (Thangamani & Bhuvaneshwari, 2022).

Fourier Transform Infrared (FT-IR):

The characterization of groups related to different compounds in the bacterial CFF and their involvement in the reduction, capping, and stabilization of Ag-NPs was conducted using FT-IR spectroscopy. FTIR with the model of Cary 630 was utilized to achieve this analysis within a wavenumber of 400–4000 cm^{-1}.

X-ray Diffraction (XRD):

The X-ray apparatus (X'Pert, Philips, Eindhoven, Netherlands) was used to investigate the nature of nano-Ag within the 2θ range of 5° to 80°. The source of X-ray radiation was Ni-filtered Cu Ka with a voltage of 40 kV and a current of 30 mA. The determination of the average size of Ag-NPs synthesized by bacterial strain Af.15 was

achieved using the Scherrer equation as outlined below (Hossain et al., 2022):

$$Crystallite \text{ average size} = \frac{0.94\lambda}{\beta \cos\theta} \qquad (1)$$

Where 0.94, λ, β, and θ are the Scherrer's constant, the wavelength of the X-ray used, the half of the maximum intensity, and the Bragg's angle respectively.

Dynamic Light Scattering and Zeta Potential Analysis:

The assessment of the distribution and hydrodynamic sizes in the colloidal solution utilized dynamic light scattering (DLS) on the Nano-ZS instrument from Malvern Ltd, Malvern, UK. To prevent any interference in the signal during analysis, the Ag-NPs were suspended in high-purity H_2O. Additionally, the surface charge of the synthesized Ag-NPs was determined using the Zetasizer apparatus (Nano-ZS, Malvern, UK) (Abdel-Rahman A. Nassar, Atta, Abdel-Rahman, El Naghy, & Fouda, 2023).

Mosquito Rearing:

The *Culex pipiens* eggs were obtained from the Medical Entomology Institute in Giza, Egypt, and promptly transferred to the Mosquito Lab., Al-Azhar University, Cairo, Egypt. The eggs were incubated under optimal conditions (Temp., 27 ± 2 °C, humidity, 75–85%, and photoperiod: 14:10 hours light-dark) in Cup filled with 0.5 L tap H_2O until they hatched. The feeding of larvae was achieved on yeast hydrolysate: dog biscuits in a per cent 1:3 ratio (w/w). Once pupae had emerged, they transferred to a second cup containing 0.5 L of dechlorinated H_2O and placed on a chiffon cage (90 x 90 x 90 cm^3) until the adults emerged, which were subsequently fed a 10% (v/v) sucrose solution (Awad et al., 2022). The experiment to study the toxicity of the synthesized nano-Ag was applied to collected larvae and pupae.

Measurement of Ag-NPs Toxicity Against Larvae and Pupae:

The larvae (I, II, III, and IV instars) as well as the pupae of *C. pipiens* were used to investigate the toxicity of biogenic Ag-NPs. The assessment was achieved through the mixing of nano-Ag with distilled H_2O at concentrations of 10, 15, 20, 25, and 30 ppm. The growth patterns, body proportions change, head width, colouration, and body segment parts were used as the main characteristics to differentiate between insect instars. To explore these differences, 25 larvae or pupae were incubated overnight in a glass cup containing 0.5 L of dechlorinated H_2O, supplemented with the designated concentration of nano-Ag and 0.5 mg of larval food. This experiment was conducted separately for each larval instar and for the pupae, with the specified nanoparticle concentration, and was repeated three times for accuracy. (Ayubi, Moravvej, Karimi, & Jooyandeh, 2013). A control group, consisting of larvae and pupae in the same above solution without NPs, was maintained under the same conditions.

Mortality percentages were calculated after 24, 48, and 72 hours using the following equation:

$$Mortality\ \% = \frac{NT}{NC}\ x\ 100$$

Where NT and NC are the numbers of treated and control individuals respectively.

Biochemical Parameters Analysis:

Following a 24-hour treatment period, the larvae were picked up from the solution and rinsed with cold saline. A 10% tissue homogenate of the larvae was prepared using a homogenizer in a chilled sucrose solution (0.25M). This homogenate was then centrifuged at 700 rpm for 10 minutes to eliminate cellular debris. The resulting supernatant was utilized for the quantification of total carbohydrates, lipids, and proteins, as well as alkaline and acid phosphatase activities. All biochemical assessments were conducted in triplicate.

Assessment of Total Proteins:

The protein contents in the larvae extract were estimated by Lowry's method. Folin-

Coicalteu will react with larvae protein to form purple blue color which estimated their intensity by reading its absorbance at 620 nm (Lowry, Rosebrough, Farr, & Randall, 1951).

Assessment of Total Carbohydrates:

Carbohydrate Estimation Procedure:

Carbohydrate levels were determined following the method outlined by Nelson (Nelson, 1944). Initially, proteins were precipitated out of the tissue homogenate, leaving a filtrate that contained glucose as the reducing sugar. This filtrate was then reacted with an alkaline copper reagent and subsequently treated with an Arsenomolybdate reagent. The resulting blue colour was measured at an absorbance of 540 nm, allowing for the quantification of the carbohydrate content.

Lipids Estimation:

Method outline by Entenman (Entenman, 1957) was utilized to estimate the total lipids that exist in the extract. The chloroform-methanol solution was used to separate the lipid content from the non-lipid. A sulphuric acid dichromate mixture was used to reduce lipids in the tissue extract that were found in the aqueous phase. The resultant green color was measured at 600 nm and the concentration of lipid was calculated.

Data Analysis:

The SPSS software (version 16.0) was used to statistically analyse the collected data. For the laboratory assays on acute toxicity, the data were first transformed into arcsine proportions and then analyzed using a two-way ANOVA, considering dosage and mosquito instar as the two factors. Additionally, the mortality data for insect pests were subjected to probit analysis, and the LC50 and LC90 values were calculated following Finney's method (Mocroft *et al.,* 1998).

RESULTS AND DISCUSSION

Endophytic Bacterial Strain Mediated Biosynthesis of Ag-NPs:

The production of Ag-NPs by endophytic bacterial strains is an exciting new direction in nanotechnology with clear advantages over more conventional chemical and physical synthesis methods. Producing NPs using endophytic bacteria, which exist within plant tissues, is an environmentally friendly method (Salem & Fouda, 2021). The elimination of potentially harmful chemicals and high-energy uses means less of an influence on the environment, making this a major plus (Mayegowda *et al.,* 2023). The endophytic bacterial strains serve as natural bioreactors, catalysing the reduction of silver ions and the consequent creation of nanoparticles through their metabolic processes. The use of endophytic bacterial strains offers a sustainable alternative with inherent biocompatibility (Eid *et al.,* 2021). This biological synthesis method yields Ag-NPs with less cytotoxicity, making them more broadly applicable in the biomedical field. This is a major benefit compared to chemically synthesised nanoparticles, which may require the addition of stabilising agents or capping agents, both of which raise safety concerns (Bogas et al., 2022). Furthermore, the endophytic bacterial strain-mediated NPs synthesis also coincides with the growing desire for green and sustainable practices in nanotechnology. The biosynthesis process occurs under mild reaction conditions, reducing energy consumption and minimizing the overall environmental footprint associated with nanoparticle production (Rahman *et al.,* 2019). Additionally, the use of naturally occurring bacterial strains introduces an element of biocompatibility that is crucial for applications such as drug delivery, where compatibility with biological systems is paramount (Eid *et al.,* 2020).

Herein, the bacterial endophytic strain, *Brevibacillus agri* Af.15 which was isolated from the medical plant *Achillea fragrantissima* was used to fabricate nano-Ag. The change of CFF colour to yellowish-brown was considered the first sign of successful formation. The

change of colour was related to surface plasmon resonance (SPR) excitation. This phenomenon occurs due to the collective oscillation of free electrons on the nanoparticle's surface when they are exposed to light (Soliman *et al.*, 2021). Upon the reduction of Ag, ions occur to form Ag-NPs that exhibit unique optical properties, specifically the absorption and scattering of light, which contribute to the observed colour change (Thangamani & Bhuvaneshwari, 2022).

Ag-NPs Characterization:

UV-Vis Spectroscopy:

The intensity of colour change was measured at varied wavelengths to detect the maximum SPR for the synthesized Ag-NPs. As shown, the UV analysis revealed a distinct SPR manifested by a well-defined peak at 425 nm (Fig. 1). This spectral feature is indicative of the spherical shape characteristic of the synthesized Ag-NPs as mentioned previously (Lee *et al.*, 2018; Wypij *et al.*, 2018). Previous studies have linked the spherical morphology of Ag-NPs to the occurrence of a SPR peak in the 410–450 nm region (Salem et al., 2020; Zaheer & Rafiuddin, 2012). Similarly, the SPR of Ag-NPs produced by the action of metabolites of *Bacillus cereus* strain A1-5, *Streptomyces noursei* strain H1-1, and *Rhizopus stolonifera* strain A6-2 was observed at 420 nm (Alsharif e*t al.*, 2020). Also, the maximum SPR of *Zingiber officinale that* produces Ag-NPs was localized at 425 nm (Vijaya et al., 2017). Dong and co-authors indicate the typical SPR peak for nano-synthesized Ag through green methods fell within the wavelength 400–450 nm range (Dong *et al.*, 2017). Any deviation in the SPR peak could be related to different biomolecules that have dual reducing and capping functions.

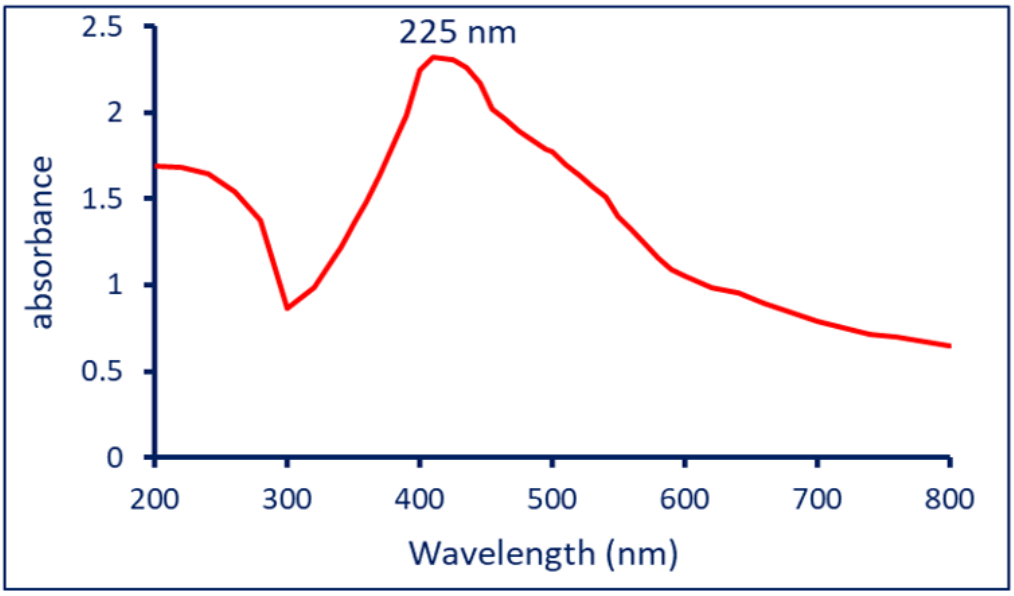

Fig. 1: UV-Vis analysis of Ag-NPs formed by bacterial strain Af15 exhibits the SPR at 225 nm.

SEM and EDX:

The shape, surface morphology, NP sizes, and as-formed sample elemental components were detected using SEM and EDX. SEM is a useful technique that can be used to assess the nano-Ag size and shape. SEM provides high-resolution images, allowing for the visualization of surface morphology and details of nanoscale structures (Khan, Saeed, & Khan, 2019). As shown, the synthesized Ag-NPs were spherical in shape, well arranged, and had sizes in the ranges of 20 - 50 nm (Fig. 2A). Recently, the Ag-NP sizes produced by pomegranate peel extract were less than 100 nm (Goudarzi, Mir, Mousavi-Kamazani,

Bagheri, & Salavati-Niasari, 2016). The elementary mapping of biosynthesized Ag-NPs was assessed using EDX analysis as shown in Figure 2B. Data analysis showed that the primary constituent of the synthesized material is Ag, with weight and atomic percentages of 46.20% and 13.96%, respectively. EDX chart exhibits a strong peak for Ag compared to the weak signals for other compounds, indicating the Ag ions reduction to elemental Ag (Jyoti, Baunthiyal, & Singh, 2016). Cu's EDX peak is an artefact of the Cu-grid that was used to cover the sample. The EDX analysis detected the presence of other elements in the sample, including O, C, N, P, Na, Al, P, Mo, Cl, K, and Ca, with low weight and atomic percentages (Fig. 2B). These elements could originate from the scattering of various biomolecules from the bacterial strain or the growth medium used in the synthesis process (Femi-Adepoju, Dada, Otun, Adepoju, & Fatoba, 2019; Fouda, Awad, et al., 2022). Given the wide range of elements present, it is likely that many different biomolecules work together to reduce, cap, and stabilise the Ag-NPs. Similarly, the EDX analysis of nano-Ag fabricated by *Gleichenia pectinata* indicates the presence of Ag in addition to other elements such as O, Si, Al, and K with varied weight percentages (Femi-Adepoju *et al.*, 2019). The authors suggested that the presence of these elements is due to biomolecules in the plant aqueous extract. Also, the Ag element represented the major component of Ag-NPs fabricated by bacterial strain *B. cereus* with weight percentages of 46.0%, additionally the presence of other weak peaks corresponding to the O, C, Pb, Na, Ca, Cl, P, and Mg (Alsharif *et al.*, 2020).

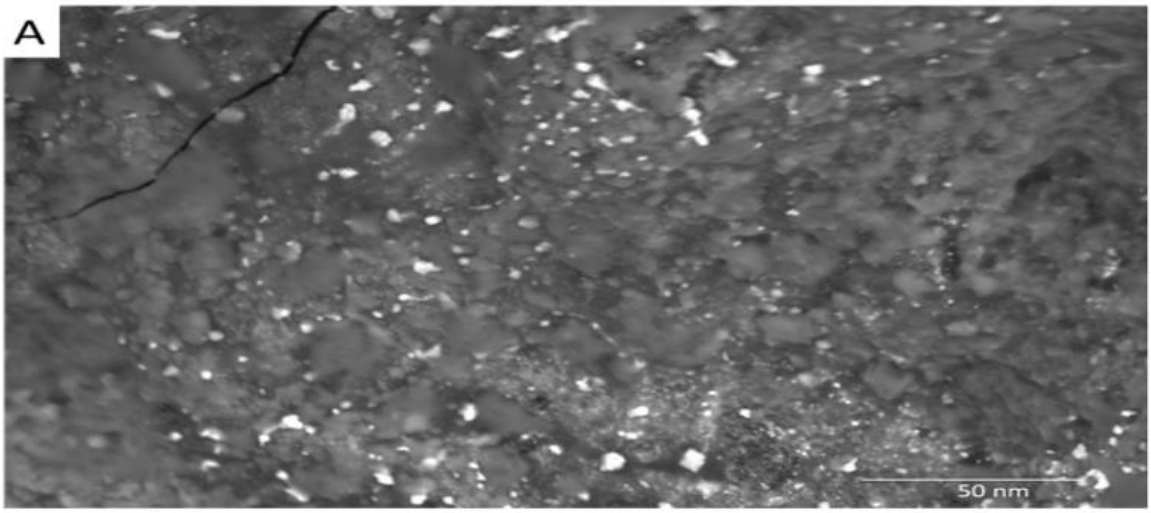

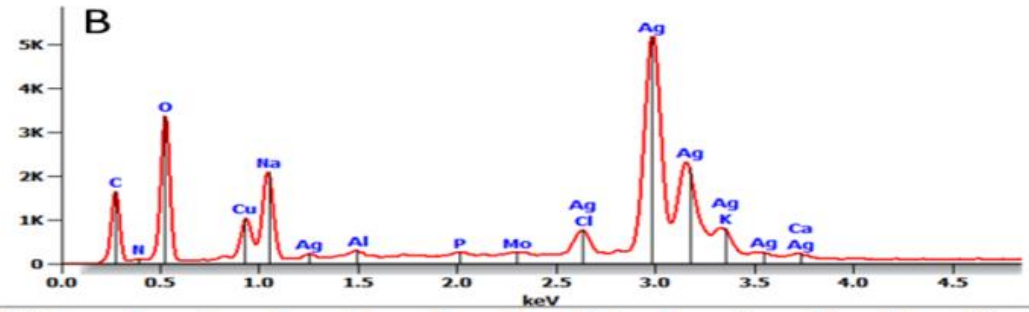

Element	C	N	O	Na	Al	P	Mo	Cl	K	Ca	Cu	Ag
Weight (%)	4.54	0.62	25.98	7.21	0.40	0.22	0.62	1.27	0.71	0.46	11.76	46.20
Atomic (%)	12.32	1.43	52.94	10.23	0.49	0.24	0.21	1.17	0.59	0.38	6.04	13.96

Fig. 2: A is the SEM image of bacterial synthesized Ag-NPs, and B is the EDX analysis showing the components of the as-formed compound.

FT-IR:

The functional groups related to biomolecules in CFF utilized to form nano-Ag were investigated by FT-IR. As shown the FT-IR of CFF contains three peaks at 3404, 2050, and 1632 cm^{-1} (Fig. 3). The broadness peak at 3404 cm^{-1} signifies to N–H and O–H stretching of amino acids and proteins (Mohammed F. Hamza et al., 2022). This peak was changed to a wavenumber of 3410 cm^{-1} after nano-Ag fabrication. The peak at a wavenumber of 2050 cm^{-1} corresponding to aromatic compounds overlapped with the vibration of the ν(C-O) (Hamza *et al.*, 2021). The peak at 1632 cm^{-1} related to the C=O and C=N stretching amides, as well as related to the N-H in primary amines (Coates, 2000), shifted to 1639 cm^{-1} upon forming nano-Ag. The other at wavenumbers of 1382, 1078, and 777 cm^{-1} were shown in FT-IR spectra of Ag-NPs. The stretching OH and NH of secondary amines overlapped with the binding CH were observed at a wavenumber of 1382 cm^{-1} (Abdel-Maksoud et al., 2023; Ghosh, Roy, Naskar, & Kole, 2023). On the other hand, the peaks at 1078 cm^{-1} and 777 cm^{-1} correspond to the stretching CN of amines and stretching C-Cl of halo compound respectively (Coates, 2000; Mohammed F Hamza *et al.*, 2022). According to the presented evidence, proteins, amines, amino acids, and amides play a crucial role in the reduction, stabilization, and dispersion of biosynthesized Ag-NPs. As a result, it is reasonable to deduce that the various metabolites found in the biomass filtrates of endophytic bacterial strain Af.15 play a significant role in the production and size reduction of Ag, leading to well-stabilized nano-formations. This complex interaction between metabolites will likely affect the biosynthesized nanoparticles' functional characteristics and potential uses.

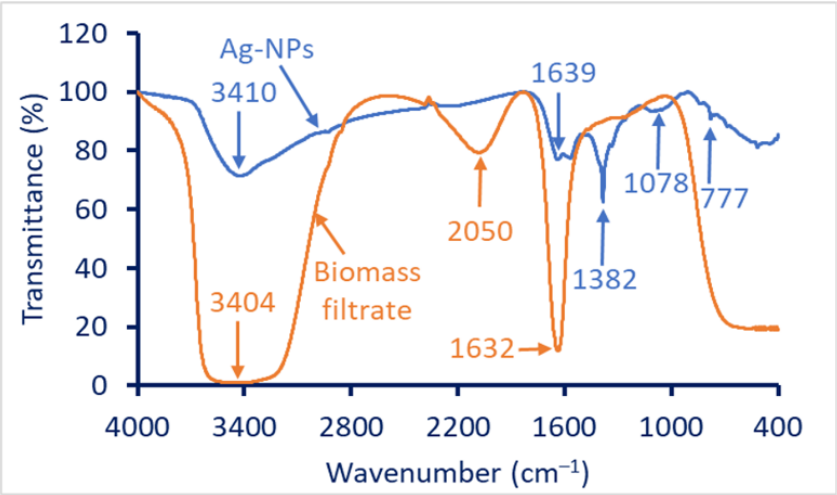

Fig. 3. FT-IR of CFF of endophytic bacterial strain AF.15 and biosynthesized nano-Ag showed the presence of various functional groups.

XRD:

The structure of bacterially formed nano-Ag was examined using XRD analysis, which was analyzed at 2θ values ranging from 5° to 80° (Fig. 4). The XRD pattern revealed four prominent diffraction peaks at 2θ values of 38.06°, 44.3°, 64.1°, and 77.34°, corresponding to the (111), (200), (220), and (311) planes, respectively. These results align with reference number 04-0783 of the Joint Committee on Powder Diffraction Standards (JCPDS), confirming that the produced nano-Ag possess a face-centred cubic structure, indicative of their crystallographic nature (Awad *et al.*, 2022; Vijayabharathi, Sathya, & Gopalakrishnan, 2018). This data was in agreement with various studies concerning the synthesis of Ag-NPs using different biological entities (Femi-Adepoju *et al.*, 2019; Rahman *et al.*, 2019; Vijayabharathi *et al.*, 2018). The weak XRD signals could be related to the

metabolites of bacterial strains that act as capping agents, which is compatible with EDX analysis. The average crystallite sizes of formed nano-Ag were estimated by the Scherrer equation. Data showed that the average crystallite nano-Ag size was 55 nm. Interestingly, the average Ag-NPs crystallite size of formed by CFF of *B. cereus* A1-5 was 55 nm (Alsharif *et al.*, 2020). Whereas those formed by *Urtica dioica* leaf extract have an average crystallite size of 25 nm (Jyoti *et al.*, 2016).

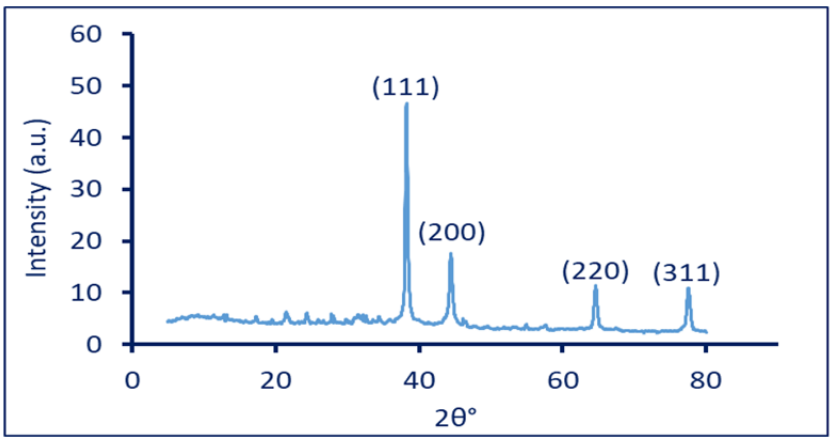

Fig. 4: Crystalline nature of nano-Ag detected by X-ray diffraction analysis.

DLS and Zeta Potential:

The size distribution of as-formed nano-Ag in colloidal solution was assessed by DLS. The analysis revealing a particle size in a colloidal solution of 58 nm for Ag-NPs synthesized by the endophytic bacterial strain *Brevibacillus agri* Af.15 is significant (Fig. 5A). This size determination provides valuable insights into the physical characteristics of the NPs. The size of NPs is a critical parameter influencing their behaviour, reactivity, and potential applications. In this case, Although the sizes obtained by DLS are higher than those of SEM and XRD, it is still relatively small and suggested that the synthesized Ag-NPs fall within the nanoscale range. The higher DLS sizes may be due to the fact that measuring sizes using DLS was achieved in a hydrated state (hydrodynamic residue) while measuring using TEM calculates the NP diameter in the solid state (Fouda, Hassan, Eid, Abdel-Rahman, & Hamza, 2022; Mollick *et al.*, 2019). Additionally, DLS can be influenced by coating agents and non-homogeneous distribution, leading to an increase in recorded sizes (Fouda, Al-Otaibi, *et al.*, 2022; Abdel-Rahman A Nassar, Eid, Atta, El Naghy, & Fouda, 2023). The DLS analysis indicating a particle size of 58 nm provides information on the homogeneity and stability of the synthesized Ag-NPs in the colloidal solution.

However, NPs of this size have a number of desirable characteristics that make them useful in many fields, including the medical and chemical sciences. Due to their diminutive stature, they boast a larger surface area in comparison to their size; this makes them more reactive in biological settings and has the potential to boost their catalytic efficacy. Improved cellular penetration and absorption by nanoparticles in this size range is particularly important for medication administration and imaging applications (Altammar, 2023).

The Ag-NPs are stable in the colloidal solution, as indicated by their measured zeta potential of –19 mV (Fig. 5B). A rise in the absolute value of the zeta potential (either positive or negative) signifies an increase in the electrostatic repulsion between particles, leading to greater stability. Because particles with like charges are repelled by each other, agglomeration and precipitation are prevented when the zeta potential is negative (Bhattacharjee, 2016).

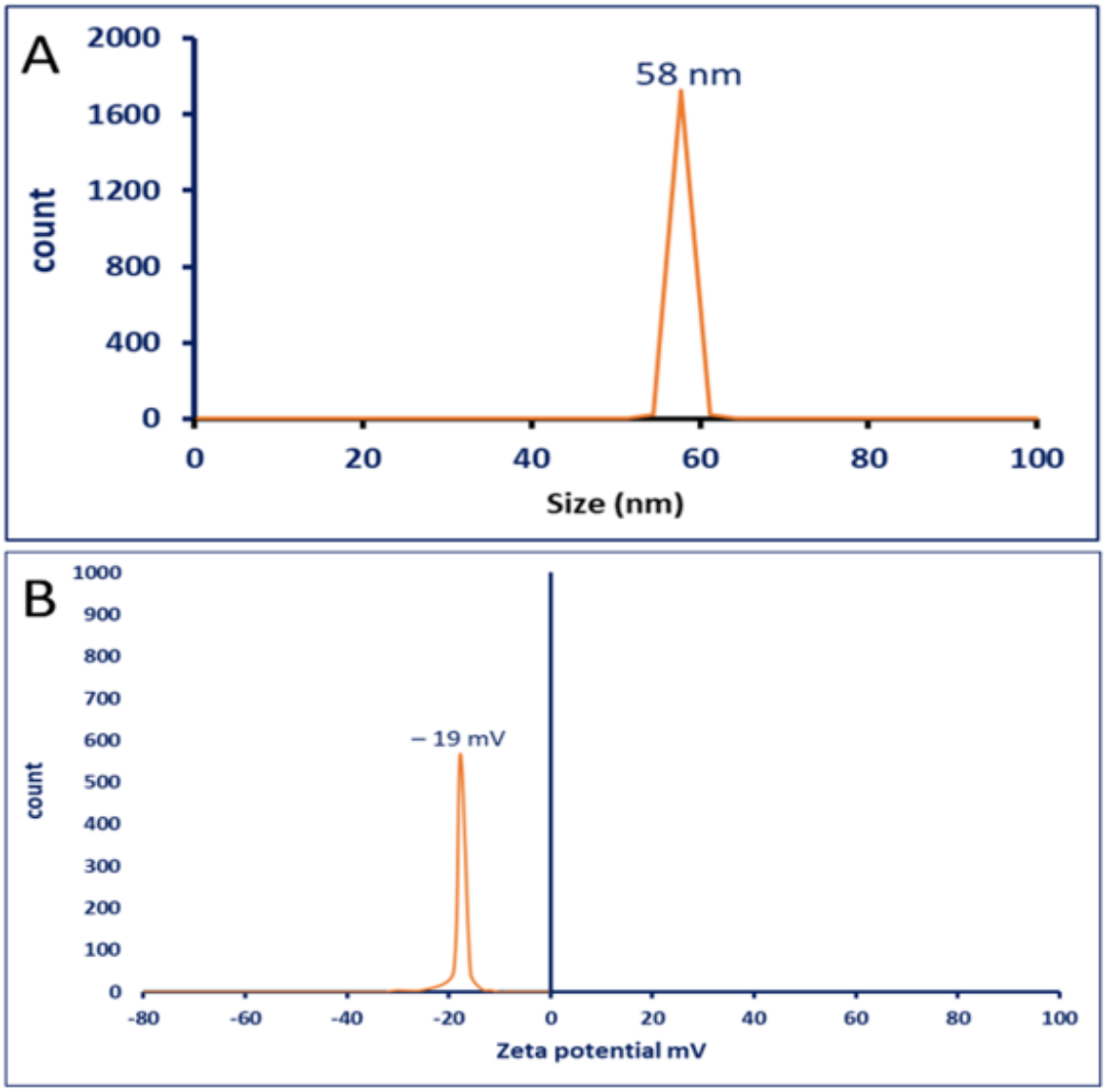

Fig. 5: A is a dynamic light scattering of biosynthesized Ag-NPs showing the average sizes in the colloidal solution was 58 nm, and B is the zeta potential analysis showing the surface of Ag-NPs bearing a negative charge.

Larvicidal Activity:

The mortality rate for *Culex pipiens* mosquito larvae in I, II, III, and IV larval instars as well as their pupal stage was determined by applying WHO recommendations. Percentage of dead pupae and instars I, II, III, and IV subjected to varying doses (10, 15, 20, 25, and 30 ppm) of nano-Ag produced by the bacterial strain *Brevibacillus agri* as shown in (Table 1). For the I, II, III, and IV instars, the corresponding LC_{50} (LC_{90}) values were 16.34 (30.74), 17.19 (36.59), 21.70 (39.54), and 27.68 (51.57) ppm. In a similar vein, the pupal stage's LC_{50} and LC_{90} levels were 26.29 and 49.33 ppm. It was discovered that the toxicity or mortality inflicted upon mosquito larvae depended on the concentration. For example, it was discovered that the treated larvae's mortality rate rose as the nanoparticle concentration rose (Table 1). The outcome suggests that in order to cause toxicity against larvae in the III instar, a greater concentration is needed (Table 1). The resistance may result from the structural and functional changes that instar larvae go through as they mature. Our results are consistent with those that showed that Ag-NPs produced by fungal strains were effective at killing larvae. Moreover, the findings from this study indicate that exposing larvae to a consistent

concentration of nanoparticles (10 ppm) results in a higher mortality rate among second-instar larvae compared to third-instar larvae (Shamia, Mohan, & Srivastava, 2006). This suggests that in order to enhance mortality rates among more developed larvae in higher stages, it would be necessary to increase the nanoparticle concentration (Sharma, Mohan, & Srivastava, 2009).

Using WHO guidelines, the mortality rate for *C. pipiens* mosquito larvae in stages I, II, III, and IV as well as their pupal stage was calculated. for samples exposed to different dosages of silver nanoparticles made by the bacterial strain *Brevibacillus agri* (10, 15, 20, 25, and 30 ppm).

Table 1. Larvicidal and pupicidal activity of filaria vector mosquito by biosynthesized Ag-NPs from endophytic bacterial strain, Brevibacillus agri

Mosquito stage	**Mortality percentage of larvae and pupae ± SD***						
Conc.	10 ppm	15 ppm	20 ppm	25 ppm	30 ppm	Lc_{50}(ppm) (LFL-UFL)	$Lc9_0$(ppm) (LFL-UFL)
I instar	32±0.41	46.2±0.31	62.0±0.87	72.2±0.13	88.4±0.95	16.34 (14.12-18.63)	30.74 (28.30-31.01)
II instar	28.1±0.03	56.3±0.71	55.2±0.09	63.0±1.12	76.3±0.81	17.19 (13.11-19.68)	36.59 (31.29-37.22)
III instar	25.1±1.10	32.0±0.19	49.1±0.69	55.1±1.19	69.6±1.12	21.70 (17.79-22.66)	39.54 (36.62-39.95)
IV instar	20.4±0.32	26.2±1.22	40.5±1.00	46.5±0.99	52.1±1.41	27.68 (23.59-27.58)	51.57 (45.19-51.46)
Pupa	14 ±0.61	20.1±0.31	30.1±1.71	40.3±1.63	47.3±1.01	26.29 (24.12-29.32)	49.33 (45.99-51.68)

Number of tested larvae = 25 per one replicate; Conc. = Concentration; All data represented as Mean ± SD.

Biochemicals Assessment:

Table 2 shows the amount of protein in the tissues of III instar larvae subjected to varying doses of Ag NPs. It was discovered that the treated larvae's estimated protein content had dropped, which may have a direct bearing on the death rate. Increased toxicity leads to a large downregulation of protein content because it lowers the protein level in mosquito larvae (Table 2). A change in protein metabolism may result from stress placed on the larvae, which either boosts or decreases their ability to synthesize proteins for energy. This demonstrates that the production of proteins is dominated by proteolysis under stress. This may be caused by the degradation of protein into amino acids (Nath, Suresh, Varma, & Kumar, 1997). Consequently, upon entering the TCA cycle as keto acids, these amino acids contribute to generating energy for the insect (Nath *et al.*, 1997). Therefore, depletion in the protein tissues from physiological mechanisms and may contribute to compensatory mechanisms that maintain hemolymph's free amino acid content during insecticidal stress, thereby providing intermediates for the Krebs cycle (Murray, Granner, Mayes, & Rodwell, 2003). Our findings are consistent with those reported that *Culex* larvae treated insecticidally with eucalyptus oil nanoemulsion had lower protein content (Sugumaran, 2010).

The protein content in the larval tissues was significantly decreased upon exposure to manufactured Ag nanoparticle-induced toxicity in a concentration-dependent manner (Gäde, 2004). This indicates that disruption of the metabolism of carbohydrates has a positive effect on nanoparticle therapy. During stress, fat bodies' glycogen stores are the primary source of carbohydrates, which leads to an increase in the amount of soluble carbohydrates in hemolymph (Gäde, 2004). The polysaccharides are broken down using insects into simple sugars which absorb glucose in the midgut, which immediately raises the hemolymph's glucose concentration. Glycolysis uses some of the glucose directly, converts some into trehalose, and stores the remainder as glycogen in the fat body (Lum & Chino,

1990). Additionally, it is consistent with research that confirmed the effects of derivative from benzoyl phenyl urea on *Culex pipiens* larvae (Djeghader, Hamid, Bouaziz, & Soltani, 2013).

The third instar larvae exhibit a considerable reduction in lipid levels upon treatment with Ag NP. This decrease was inversely correlated with both mortality and Ag NP concentration. In addition to their importance in the cell's membrane made up, lipids have various important such as its necessary for reproduction, maintenance, and development of embryos. The cholesterol levels decrease may be attributed to reduce the synthesis of lipids and the mobilization of stored lipids, which occur as lipid molecules progressively unsaturated (Mulye & Gordon, 1993). Our findings support the findings of Senthilkumar and coauthors, who showed that *Anoepheles stephensi* larvae treated with several plant-based insecticidal formulations experienced a decrease in total lipid levels, hence causing stress to the larval species (Senthilkumar, Varma, & Gurusubramanian, 2009).

Table 2: Protein, carbohydrate, and lipid content in III Instar larvae of filaria vector mosquito by biosynthesized Ag-NPs from endophytic bacterial strain, Brevibacillus agri

Ag-NPs	Protein (µg/g)	Carbohydrate (µg/g)	Lipid (µg/g)
control	172.1 ± 4.31	118.1±4.61	463.1±1.32
10 ppm	129.5± 1.41	128.4±4.89	402.1±3.16
15 ppm	107.4± 4.21	148.5±4.34	341.3±5.71
20 ppm	91.4± 1.82	175.6±4.13	301.2±6.34
25 ppm	75.1±2.24	198.7±2.15	246.3±10.71
30 ppm	54.2±1.72	91.3±2.17	204.6±9.31

Conclusions:

In this investigation, Ag at the nanoscale was formed using CFF of bacterial endophytes namely *Brevibacillus agri* strain Af.15. The produced nano-Ag was characterized by UV, FT-IR, SEM-EDX, XRD, DLS, and zeta potential which confirmed the reduction of metal precursor ($AgNO_3$) to form nanoscale structure (Ag-NPs). The biological applications of this nanoscale structure demonstrated their strong larvicidal effectiveness against various instars of *Culex pipiens* larvae and pupae as shown by percentages of mortality at different NPs concentrations and reducing in the biochemical characteristic of larvae extract (lipid, proteins, and carbohydrates). Our findings suggest that these nano-Ag could serve as effective agents for reducing *Culex pipiens* larval populations. Overall, this avenue of research holds significant potential for addressing mosquito-borne diseases by controlling the larvae and pupae in an eco-friendly, cost-effective, and rapid method.

Declarations:

Ethical Approval: Ethical Approval is not applicable.

Authors Contributions: Dr. Kotob Mohamed Hammad and Dr. Amr fouda made a great effort in the technique of the experiment. Dr. Mohamed Ahmed Awed and Mr. Mohamed Awed Allah made great efforts to breeding different the stages of Mosquito *Culex pipens* in this experiment. Dr. Kotb Mohamed Hammad, Mr. Mohamed A. Ahmed, Dr. Mohamed A. Awad and Amr Fouda were a major contributor to the manuscript writing. Dr. Ahmed saber Bream and Dr. Ahmed Mohamed Eid made the Revion of the manuscript. All authors read and approved the final manuscript.

Competing Interests: The authors declare that they have no competing interests.

Availability of Data and Materials: The data supporting this study findings are available from all authors upon reasonable request.

Source of Funding: The current research was not funded.

Acknowledgements: We are grateful to Dr. Kotob Mohamed Hammad,Dr. Amr fouda and Dr. Mohamed Ahmed Doctorate at the Faculty of Science, Department of Entomology and

Microbiology, Al-Azhar University in Cairo for providing critical assistance to this study.

REFERENCES

Abdel-Maksoud, G., Abdel-Nasser, M., Hassan, S. E.-D., Eid, A. M., Abdel-Nasser, A., & Fouda, A. (2023). Biosynthesis of titanium dioxide nanoparticles using probiotic bacterial strain, Lactobacillus rhamnosus, and evaluate of their biocompatibility and antifungal activity. *Biomass Conversion and Biorefinery*, 1-23.

Al-Kubati, A. S., Al-Samie, A. R., Al-Kubati, S., & Ramzy, R. M. (2020). The story of Lymphatic Filariasis elimination as a public health problem from Yemen. *Acta Tropica, 212*, 105676.

Alkahtani, M. D. F., Fouda, A., Attia, K. A., Al-Otaibi, F., Eid, A. M., Ewais, E. E., . . . Abdelaal, K. A. A. (2020). Isolation and Characterization of Plant Growth Promoting Endophytic Bacteria from Desert Plants and Their Application as Bioinoculants for Sustainable Agriculture. *Agronomy, 10*(9). Retrieved from doi:10.3390/agronomy10091325

Alsharif, S. M., Salem, S. S., Abdel-Rahman, M. A., Fouda, A., Eid, A. M., El-Din Hassan, S., . . . Mohamed, A. A. (2020). Multifunctional properties of spherical silver nanoparticles fabricated by different microbial taxa. *Heliyon, 6*(5), e03943. doi:10.1016/j.heliyon.2020.e03943

Altammar, Khadijah A. (2023):"A review on nanoparticles: characteristics, synthesis, applications, and challenges." *Frontiers in microbiology* 14 1155622.

Awad, M. A., Eid, A. M., Elsheikh, T. M., Al-Faifi, Z. E., Saad, N., Sultan, M. H., . . . Fouda, A. (2022). Mycosynthesis, characterization, and mosquitocidal activity of silver nanoparticles fabricated by Aspergillus niger strain. *Journal of Fungi, 8*(4), 396.

Ayubi, A., Moravvej, G., Karimi, J., & Jooyandeh, A. (2013). Lethal effects of four insecticides on immature stages of Chrysoperla carnea (Stephens)(Neuroptera: Chrysopidae) in laboratory conditions. *Turkish Journal of Entomology, 37*(4), 399-407.

Benelli, G. (2015). Research in mosquito control: current challenges for a brighter future. *Parasitology research, 114*(8), 2801-2805.

Benelli, G., & Mehlhorn, H. (2016). Declining malaria, rising of dengue and Zika virus: insights for mosquito vector control. *Parasitology research, 115*, 1747-1754.

Bhattacharjee, S. (2016). DLS and zeta potential–what they are and what they are not? *Journal of controlled release, 235*, 337-351.

Bogas, A. C., Henrique Rodrigues, S., Gonçalves, M. O., De Assis, M., Longo, E., & Paiva De Sousa, C. (2022). Endophytic Microorganisms From the Tropics as Biofactories for the Synthesis of Metal-Based Nanoparticles: Healthcare Applications. *Frontiers in Nanotechnology, 4*. doi:10.3389/fnano.2022.823236

Chen, Y.-T., Yuan, Q., Shan, L.-T., Lin, M.-A., Cheng, D.-Q., & Li, C.-Y. (2013). Antitumor activity of bacterial exopolysaccharides from the endophyte Bacillus amyloliquefaciens sp. isolated from Ophiopogon japonicus. *Oncology letters, 5*(6), 1787-1792.

Chowdhury, Soumitra Paul, *et al.* (2015):"Biocontrol mechanism by root-associated Bacillus amyloliquefaciens FZB42–a review." *Frontiers in microbiology* 6 780.

Coates, J. (2000). Interpretation of infrared spectra, a practical approach, In Encyclopedia of Analytical Chemistry; John Wiley & Sons USA,: Ltd.: Hoboken, NJ,.

De-Jian, S., Xu-Li, D., & Ji-Hui, D. (2013). The history of the elimination of lymphatic filariasis in China. *Infectious diseases of poverty, 2*, 1-9.

Djeghader, N. E. H., Hamid, B., Bouaziz, A., & Soltani, N. (2013). Biological effects of a benzoylphenylurea derivative (Novaluron) on larvae of Culex pipiens (Diptera: Culicidae). *Advances in Applied Science Research*, 4(4):449-456

Dong, Z. Y., Narsing Rao, M. P., Xiao, M., Wang, H. F., Hozzein, W. N., Chen, W., & Li, W. J. (2017). Antibacterial activity of silver nanoparticles against Staphylococcus warneri synthesized using endophytic bacteria by photo-irradiation. *Frontiers in microbiology*, *8*, 1090.

Eid, A. M., Fouda, A., Abdel-Rahman, M. A., Salem, S. S., Elsaied, A., Oelmüller, R., . . . Hassan, S. E. (2021). Harnessing Bacterial Endophytes for Promotion of Plant Growth and Biotechnological Applications: An Overview. *Plants (Basel), 10*(5). doi:10.3390/plants10050935

Eid, A. M., Fouda, A., Niedbała, G., Hassan, S. E., Salem, S. S., Abdo, A. M., . . . Shaheen, T. I. (2020). Endophytic Streptomyces laurentii Mediated Green Synthesis of Ag-NPs with Antibacterial and Anticancer Properties for Developing Functional Textile Fabric Properties. *Antibiotics (Basel), 9*(10). doi:10.3390/ antibiotics 9100641

Femi-Adepoju, A. G., Dada, A. O., Otun, K. O., Adepoju, A. O., & Fatoba, O. P. (2019). Green synthesis of silver nanoparticles using terrestrial fern (Gleichenia Pectinata (Willd.) C. Presl.): characterization and antimicrobial studies. *Heliyon*, Volume 5, Issue 4, April 2019, e01543

Fouda, A., Al-Otaibi, W. A., Saber, T., AlMotwaa, S. M., Alshallash, K. S., Elhady, M., . . . Abdel-Rahman, M. A. (2022). Antimicrobial, antiviral, and in-vitro cytotoxicity and mosquitocidal activities of Portulaca oleracea-based green synthesis of selenium nanoparticles. *Journal of Functional Biomaterials, 13*(3), 157.

Fouda, A., Awad, M. A., Al-Faifi, Z. E., Gad, M. E., Al-Khalaf, A. A., Yahya, R., & Hamza, M. F. (2022). Aspergillus flavus-Mediated Green Synthesis of Silver Nanoparticles and Evaluation of Their Antibacterial, Anti-Candida, Acaricides, and Photocatalytic Activities. *Catalysts, 12*(5). Retrieved from doi:10.3390/ catal 12050462

Fouda, A., Hassan, S. E.-D., Eid, A. M., Abdel-Rahman, M. A., & Hamza, M. F. (2022). Light enhanced the antimicrobial, anticancer, and catalytic activities of selenium nanoparticles fabricated by endophytic fungal strain, Penicillium crustosum EP-1. *Scientific Reports*, *12*(1), 11834.

Gäde, G. (2004). Regulation of intermediary metabolism and water balance of insects by neuropeptides. *Annual Reviews in Entomology, 49*(1), 93-113.

Ghosh, S., Roy, S., Naskar, J., & Kole, R. K. (2023). Plant-Mediated Synthesis of Mono- and Bimetallic (Au–Ag) Nanoparticles: Future Prospects for Food Quality and Safety. *Journal of Nanomaterials, 2023*.

Goudarzi, M., Mir, N., Mousavi-Kamazani, M., Bagheri, S., & Salavati-Niasari, M. (2016). Biosynthesis and characterization of silver nanoparticles prepared from two novel natural precursors by facile thermal decomposition methods. *Scientific Reports*, *6*(1), 32539. doi:10.1038/srep32539

Hamza, M. F., Fouda, A., Wei, Y., El Aassy, I. E., Alotaibi, S. H., Guibal, E., & Mashaal, N. M. (2022). Functionalized biobased composite for metal decontamination–Insight on uranium and application to water samples collected from wells in mining areas (Sinai, Egypt). *Chemical Engineering Journal, 431*, 133967.

Hamza, M. F., Hamad, D. M., Hamad, N. A., Abdel-Rahman, A. A. H., Fouda, A., Wei, Y., . .El-Etrawy, A.-A. S. (2022). Functionalization of magnetic chitosan microparticles for high-performance removal of chromate from aqueous solutions

and tannery effluent. *Chemical Engineering Journal, 428*, 131775. doi:https://doi.org/10.1016/j.cej.2021.131775

Hamza, M. F., Salih, K. A. M., Abdel-Rahman, A. A. H., Zayed, Y. E., Wei, Y., Liang, J., & Guibal, E. (2021). Sulfonic-functionalized algal/PEI beads for scandium, cerium and holmium sorption from aqueous solutions (synthetic and industrial samples). *Chemical Engineering Journal, 403*, 126399. doi:https://doi.org/10. 1016/j. cej. 2020.126399

Hossain, M. S., Mahmud, M., Mobarak, M. B., Sultana, S., Shaikh, M. A. A., & Ahmed, S. (2022). New analytical models for precise calculation of crystallite size: application to synthetic hydroxyapatite and natural eggshell crystalline materials. *Chemical Papers, 76*(11), 7245-7251. doi:10.1007/s11696-022-02377-9

Jyoti, K., Baunthiyal, M., & Singh, A. (2016). Characterization of silver nanoparticles synthesized using Urtica dioica Linn. leaves and their synergistic effects with antibiotics. *Journal of Radiation Research and Applied Sciences, 9*(3), 217-227. doi:https://doi.org/10.1016/j.jrras.2015.10.002

Khan, I., Saeed, K., & Khan, I. (2019). Nanoparticles: Properties, applications and toxicities. *Arabian Journal of Chemistry, 12*(7), 908-931. doi:https://doi.org/10.1016/j. arabjc.2017.05.011

Lee, S. J., Heo, M., Lee, D., Han, S., Moon, J.-H., Lim, H.-N., & Kwon, I. K. (2018). Preparation and characterization of antibacterial orthodontic resin containing silver nanoparticles. *Applied Surface Science, 432*, 317-323. doi:https://doi.org/10. 1016/j.apsusc.2017.04.030

Li, H., Soares, M. A., Torres, M. S., Bergen, M., & White Jr, J. F. (2015). Endophytic bacterium, Bacillus amyloliquefaciens, enhances ornamental hosta resistance to diseases and insect pests. *Journal of Plant Interactions, 10*(1), 224-229.

Lowry, O. H., Rosebrough, N. J., Farr, A. L., & Randall, R. J. (1951). Protein measurement with the Folin phenol reagent. *J biol Chem, 193*(1), 265-275.

Lum, P. Y., & Chino, H. (1990). Trehalose, the insect blood sugar, inhibits loading of diacylglycerol by lipophorin from the fat body in locusts. *Biochemical and biophysical research communications, 172*(2), 588-594.

Mayegowda, S. B., Sarma, G., Gadilingappa, M. N., Alghamdi, S., Aslam, A., Refaat, B., . . . Al-Moraya, I. S. (2023). Green-synthesized nanoparticles and their therapeutic applications: A review. *Green Processing and Synthesis, 12*(1). doi:10.1515/gps-2023-0001

Mocroft, A., Vella, S., Benfield, T., Chiesi, A., Miller, V., Gargalianos, P. e. a., . . . Phillips, A. (1998). Changing patterns of mortality across Europe in patients infected with HIV-1. *The Lancet, 352*(9142), 1725-1730.

Mollick, M. M. R., Rana, D., Dash, S. K., Chattopadhyay, S., Bhowmick, B., Maity, D., . . . Chakraborty, M. (2019). Studies on green synthesized silver nanoparticles using Abelmoschus esculentus (L.) pulp extract having anticancer (in vitro) and antimicrobial applications. *Arabian Journal of Chemistry, 12*(8), 2572-2584.

Mulye, H., & Gordon, R. (1993). Effects of two juvenile hormone analogs on hemolymph and fat-body metabolites of the eastern spruce budworm, Choristoneura fumiferana (Clemens) (Lepidoptera: Tortricidae). *Canadian Journal of Zoology, 71*(6), 1169-1174. doi:10.1139/z93-159

Murray, R. K., Granner, D. K., Mayes, P. A., & Rodwell, V. W. (2003). Harper's illustrated biochemistry. Twenty-sixth edition, Lange Medical Books/McGraw-Hill Medical Publishing Division

Muthukumaran, U., Govindarajan, M., Rajeswary, M., & Hoti, S. (2015). Synthesis and characterization of silver nanoparticles using Gmelina asiatica leaf extract against

filariasis, dengue, and malaria vector mosquitoes. *Parasitology research, 114*, 1817-1827.

Nam, H.-S., Yang, H.-J., Oh, B. J., Anderson, A. J., & Kim, Y. C. (2016). Biological control potential of Bacillus amyloliquefaciens KB3 isolated from the feces of Allomyrina dichotoma larvae. *The plant pathology journal, 32*(3), 273.

Nassar, A.-R. A., Atta, H. M., Abdel-Rahman, M. A., El Naghy, W. S., & Fouda, A. (2023). Myco-synthesized copper oxide nanoparticles using harnessing metabolites of endophytic fungal strain Aspergillus terreus: an insight into antibacterial, anti-Candida, biocompatibility, anticancer, and antioxidant activities. *BMC Complementary Medicine and Therapies, 23*(1), 261. doi:10.1186/s12906-023-04056-y

Nassar, A.-R. A., Eid, A. M., Atta, H. M., El Naghy, W. S., & Fouda, A. (2023). Exploring the antimicrobial, antioxidant, anticancer, biocompatibility, and larvicidal activities of selenium nanoparticles fabricated by endophytic fungal strain Penicillium verhagenii. *Scientific Reports, 13*(1), 9054.

Nath, B. S., Suresh, A., Varma, B. M., & Kumar, R. S. (1997). Changes in protein metabolism in hemolymph and fat body of the silkworm, Bombyx mori (Lepidoptera: Bombycidae) in response to organophosphorus insecticides toxicity. *Ecotoxicology and environmental safety, 36*(2), 169-173.

Nelson, N. (1944). A photometric adaptation of the Somogyi method for the determination of glucose. *Journal of* ***Biological Chemistry,*** *153*(2), 375-380.

World Health Organization. (2016). *Strengthening the assessment of lymphatic filariasis transmission and documenting the achievement of elimination*. World Health Organization.

Panneerselvam, C., Murugan, K., Kovendan, K., Kumar, P. M., & Subramaniam, J. (2013). Mosquito larvicidal and pupicidal activity of Euphorbia hirta Linn.(Family: Euphorbiaceae) and Bacillus sphaericus against Anopheles stephensi Liston.(Diptera: Culicidae). *Asian Pacific journal of tropical medicine, 6*(2), 102-109.

Rahman, S., Rahman, L., Khalil, A. T., Ali, N., Zia, D., Ali, M., & Shinwari, Z. K. (2019). Endophyte-mediated synthesis of silver nanoparticles and their biological applications. *Applied microbiology and biotechnology, 103*, 2551-2569.

Roni, M., Murugan, K., Panneerselvam, C., Subramaniam, J., Nicoletti, M., Madhiyazhagan, P., . . . Wei, H. (2015). Characterization and biotoxicity of Hypnea musciformis-synthesized silver nanoparticles as potential eco-friendly control tool against Aedes aegypti and Plutella xylostella. *Ecotoxicology and environmental safety, 121*, 31-38.

Salem, S. S., El-Belely, E. F., Niedbała, G., Alnoman, M. M., Hassan, S. E., Eid, A. M., . . . Fouda, A. (2020). Bactericidal and In-Vitro Cytotoxic Efficacy of Silver Nanoparticles (Ag-NPs) Fabricated by Endophytic Actinomycetes and Their Use as Coating for the Textile Fabrics. *Nanomaterials (Basel), 10*(10). doi:10.3390/nano10102082

Salem, S. S., & Fouda, A. (2021). Green synthesis of metallic nanoparticles and their prospective biotechnological applications: an overview. *Biological trace element research, 199*(1), 344-370.

Santhosh, S. B., Ragavendran, C., & Natarajan, D. (2015). Spectral and HRTEM analyses of Annona muricata leaf extract mediated silver nanoparticles and its Larvicidal efficacy against three mosquito vectors Anopheles stephensi, *Culex quinquefasciatus,* and *Aedes aegypti*. *Journal of Photochemistry and Photobiology B: Biology, 153*, 184-190.

Senthilkumar, N., Varma, P., & Gurusubramanian, G. (2009). Larvicidal and adulticidal activities of some medicinal plants against the malarial vector, Anopheles stephensi (Liston). *Parasitology research, 104*, 237-244.

Shamia, P., Mohan, L., & Srivastava, C. (2006). Impact analysis of neem kernel extracts on the developmental profile of Anopheles stephensi. *Journal of Asia-Pacific Entomology, 9*(1), 11-17.

Sharma, P., Mohan, L., & Srivastava, C. N. (2009). Anti-juvenile activity of Azadirachta indica extract on the development and morphometry of filaria vector, Culex quinquefasciatus (Diptera: Culicidae) Say. *Parasitology research, 105*, 1193-1203.

Sher, N., Alkhalifah, D. H. M., Ahmed, M., Mushtaq, N., Shah, F., Fozia, F., . . . Aboul-Soud, M. A. M. (2022). Comparative Study of Antimicrobial Activity of Silver, Gold, and Silver/Gold Bimetallic Nanoparticles Synthesized by Green Approach. *Molecules, 27*(22). Retrieved from doi:10.3390/molecules27227895

Soliman, A. M., Abdel-Latif, W., Shehata, I. H., Fouda, A., Abdo, A. M., & Ahmed, Y. M. (2021). Green approach to overcome the resistance pattern of Candida spp. using biosynthesized silver nanoparticles fabricated by Penicillium chrysogenum F9. *Biological Trace Element Research, 199*, 800-811.

Soni, N., & Prakash, S. (2014). Microbial synthesis of spherical nanosilver and nanogold for mosquito control. *Annals of microbiology, 64*, 1099-1111.

Sugumaran, M. (2010). Chemistry of cuticular sclerotization. *Advances in insect Physiology, 39*, 151-209.

Thangamani, N., & Bhuvaneshwari, N. (2022). Synthesis, characterization of Ag nanoparticles using the green approach towards degradation of environmental pollutant. *Journal of Materials Science: Materials in Electronics, 33*(12), 9155-9162. doi:10.1007/s10854-021-07188-4

Van Hop, D., Hoa, P. T. P., Quang, N. D., Ton, P. H., Ha, T. H., Van Hung, N., . . . Dao, N. T. A. (2014). Biological control of Xanthomonas oryzae pv. oryzae causing rice bacterial blight disease by Streptomyces toxytricini VN08-A-12, isolated from soil and leaf-litter samples in Vietnam. *Biocontrol Science, 19*(3), 103-111.

Vijaya, J. J., Jayaprakash, N., Kombaiah, K., Kaviyarasu, K., Kennedy, L. J., Ramalingam, R. J., . . . Maaza, M. (2017). Bioreduction potentials of dried root of Zingiber officinale for a simple green synthesis of silver nanoparticles: antibacterial studies. *Journal of Photochemistry and Photobiology B: Biology, 177*, 62-68.

Vijayabharathi, R., Sathya, A., & Gopalakrishnan, S. (2018). Extracellular biosynthesis of silver nanoparticles using Streptomyces griseoplanus SAI-25 and its antifungal activity against Macrophomina phaseolina, the charcoal rot pathogen of sorghum. *Biocatalysis and Agricultural Biotechnology, 14*, 166-171.

Wypij, M., Czarnecka, J., Świecimska, M., Dahm, H., Rai, M., & Golinska, P. (2018). Synthesis, characterization and evaluation of antimicrobial and cytotoxic activities of biogenic silver nanoparticles synthesized from Streptomyces xinghaiensis OF1 strain. *World Journal of Microbiology and Biotechnology, 34*(2), 23. doi:10.1007/s11274-017-2406-3

Zaheer, Z., & Rafiuddin. (2012). Silver nanoparticles to self-assembled films: Green synthesis and characterization. *Colloids and Surfaces B: Biointerfaces, 90*, 48-52. doi:https://doi.org/10.1016/j.colsurfb.2011.09.037